# Micro-optic lens for data storage

T.D. Milster, R.M. Trusty, M.S. Wang, F.F. Froehlich, and J.K. Erwin
Optical Sciences Center, University of Arizona, Tucson, Arizona 85721

## Abstract

We describe a new type of microlens for data storage applications that has improved off-axis performance. The lens consists of a micro-Fresnel pattern on a curved substrate. The radius of the substrate is equal to the focal length of the lens. If the pattern and substrate are thin, the combination satisfies the Abbe sine condition. Therefore, the lens is free of coma. We analyze a 0.5 numerical aperture, 0.50 mm focal length lens in detail. A 0.16 numerical aperture lens was fabricated holographically, and results are presented.

## 2. Introduction

There are several types of microlenses commonly used in optical data storage systems. The most common are molded glass and molded plastic lenses. Molded optics weigh less than conventional multiple-element designs. Typical apertures are 3.5 mm to 4.5 mm in diameter, and numerical apertures (NAs) range from 0.45 to 0.55. For optical data storage applications, the smallest molded microlenses commercially available have an entrance pupil diameter of 3.0 mm (1). There are at least two reasons to use smaller optics. If a smaller microlens is used as an objective lens, the same number of disks can fit into a smaller stack height, and volumetric storage density will increase. Secondly, if all hardware dimensions scale linearly with optics size, a reduction in lens size by some factor will allow a reduction in moving mass by that factor to the third power, since mass scales with volume. The result will be an improvement in access time.

A serious problem observed with microlens components is a limited field of view. For applications like multiple beams and galvanometric tracking servos, the spatial area that must be in focus on the disk encompasses many track widths. The required focal area does not change as the objective lens focal length becomes smaller, which implies that the angular field of view increases, as shown in Figure 1. For example, consider a system that must focus over ± 30 tracks with a 0.5 numerical aperture (NA) lens. A diffraction-limited lens with a focal length of 4.5 mm requires a ±0.61° angular field. A lens with a 1.0 mm focal length would require a ±2.8° angular field. The limiting aberration in these systems is coma. Coma is also the limiting aberration in waveguides using focused grating couplers (2). In this paper, we outline a technique that eliminates coma and dramatically improves off-axis

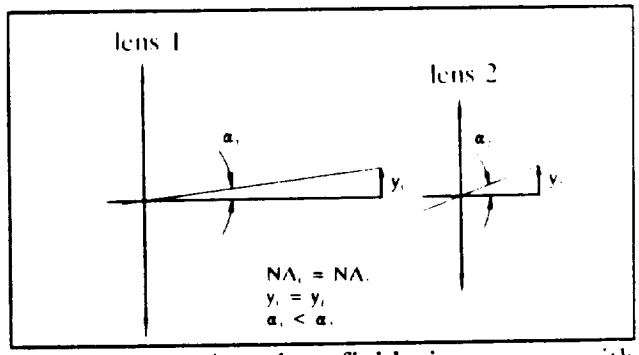


Figure 1. Angular field increases with smaller lenses.



Preprint from SPIE Proceedings Volume 1499

MILSTER

performance of these devices. A 160 $\mu$m diameter 0.16 NA microlens has been fabricated.

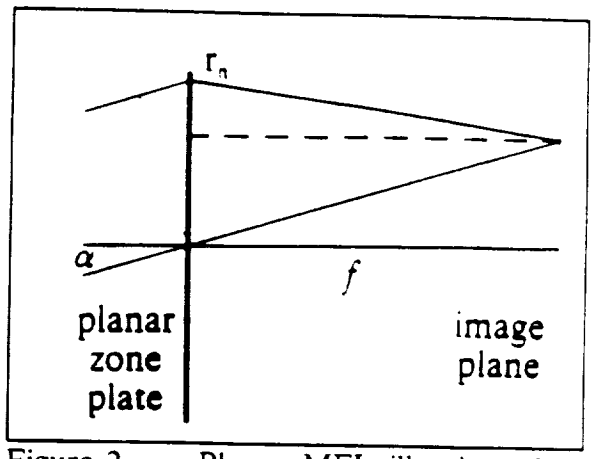


Figure 2. Planar MFL illuminated at angle $\alpha$.

## 3. Microlens properties

There are several microlens techniques which have been proposed. These include graded-index lenses (3), holographic lenses and zone plates (4), and micro-Fresnel lenses (MFLs) (5). Each of these techniques has the potential for very small apertures (~100 $\mu$m) and high NA (0.5). Graded-index lenses depend on the refraction of light rays. Holographic lenses and zone plates utilize diffraction properties. In the MFL, the center portion acts like a refractive element, and the edges (where the zone spacing is on the order of a wavelength) act like a diffractive element. The advantage of the Fresnel lens is that it does not become significantly thicker and heavier as the NA increases. We now examine the focal properties of very small (< 1 mm) focal length MFLs.

Off-axis performance of planar Fresnel lenses has been described by Young (6). Consider the geometry of Figure 2, where a planar MFL is illuminated with a plane wave at angle $\alpha$. The radius of the $n^{th}$ zone is given by $r_n$. Coma, astigmatism and field curvature aberrations are described by: $W_{131} = \alpha r_n^3/2\lambda f^2$, $W_{222} = \alpha^2 r_n^2/2\lambda f$, and $W_{220} = \alpha^2 r_n^2/4\lambda f$, respectively. These aberrations are plotted as a function of field angle, $\alpha$, in Figure 3 for the following parameters: $f$ = 1.0 mm, NA = 0.50 and $\lambda$ = 0.785 $\mu$m. This lens cannot be used at more than a 0.13° field without coma contributing $\lambda/4$ departure (Rayleigh limit) to the ideal wavefront. If the coma could be eliminated, the limiting aberration is astigmatism, which does not cross the Rayleigh limit until $\alpha \approx 2.1°$. A factor of 16 improvement in the field angle would be realized.

Coma can be eliminated by forcing the MFL to satisfy the classical Abbe sine condition (7). One way to satisfy the Abbe sine condition is make the zonal focal lengths equal when the lens is used at infinite conjugates. As shown in Figure 4, a planar MFL converts an incident plane-wave phase distribution into a converging spherical wave. The zonal focal lengths, $f_{zn}$, increase with radius. To become compatible with the Abbe sine condition, the optical power of the element can be placed on a spherical surface (8), as shown in Figure 5. The zonal focal lengths are now equal, and the Abbe sine condition is satisfied. A simple extension of Young's treatment verifies that coma is

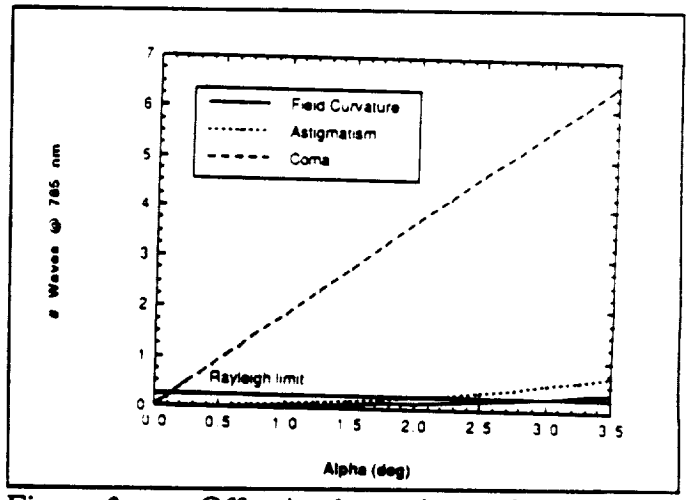


Figure 3. Off-axis aberrations of a 0.50 NA $f$ = 1.0 mm planar MFL.

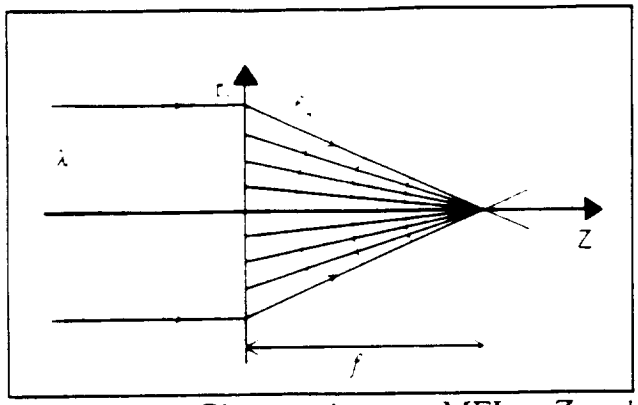


Figure 4. Planar-substrate MFL. Zonal focal lengths, $f_{zn}$, are not equal.

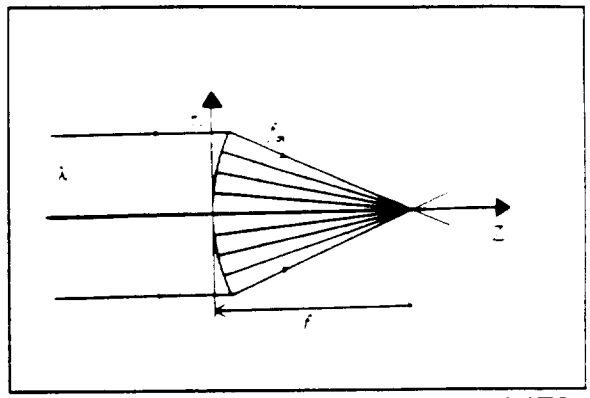


Figure 5. Curved-substrate MFL. Zonal focal lengths, $f_{zn}$, are equal.

eliminated. Delano (9) has also shown that coma is zero in this type of design.

In our treatment we neglect effects of the disk cover plate. Spherical aberration introduced by the cover plate can be corrected by modifying the MFL pattern on either the flat or curved-substrate designs. Coma due to the cover plate is small compared to coma from the flat MFL if a thin cover plate is used.

So far we have discussed properties of MFLs with the exact phase distribution required to form a converging spherical wave. The index variation is similar to a blazed and chirped diffraction grating. Blazing increases the diffraction efficiency of the MFL. Theoretically, 100% diffraction efficiency can be obtained with proper blazing (10). For the planar geometry of Figure 4, the required phase distribution is

$$\psi_n(r_n) = -\frac{2\pi}{\lambda}\left[f-\sqrt{f^2+r_n^2}\right] + n\pi \quad . \qquad [1]$$

For the curved geometry of Figure 5, the analogous expression to Equation 1 is

$$\psi_n(r_n) = -\frac{2\pi}{\lambda}\left[f-\sqrt{f^2-r^2}\right] + n\pi \quad . \qquad [2]$$

It is not necessary to form the exact phase distribution of Equation 1 or Equation 2 in order to evaluate the optical performance of the lens. Instead, a rectangular profile can be used at modulo $\pi$ phase shifts. The result is a binary-type MFL with a lower diffraction efficiency but identical optical properties. The binary-type MFLs are desirable in the initial part of the work because they are easier to fabricate.

## 4. Experiment

To date, our efforts have focused on making a micro Fresnel lens on a curved substrate. The necessary substrate must be a thin spherical shell of the proper radius and high optical quality. We modify microspheres made for laser fusion research, which have the necessary characteristics. The microspheres are available with radii in the 500 $\mu$m -

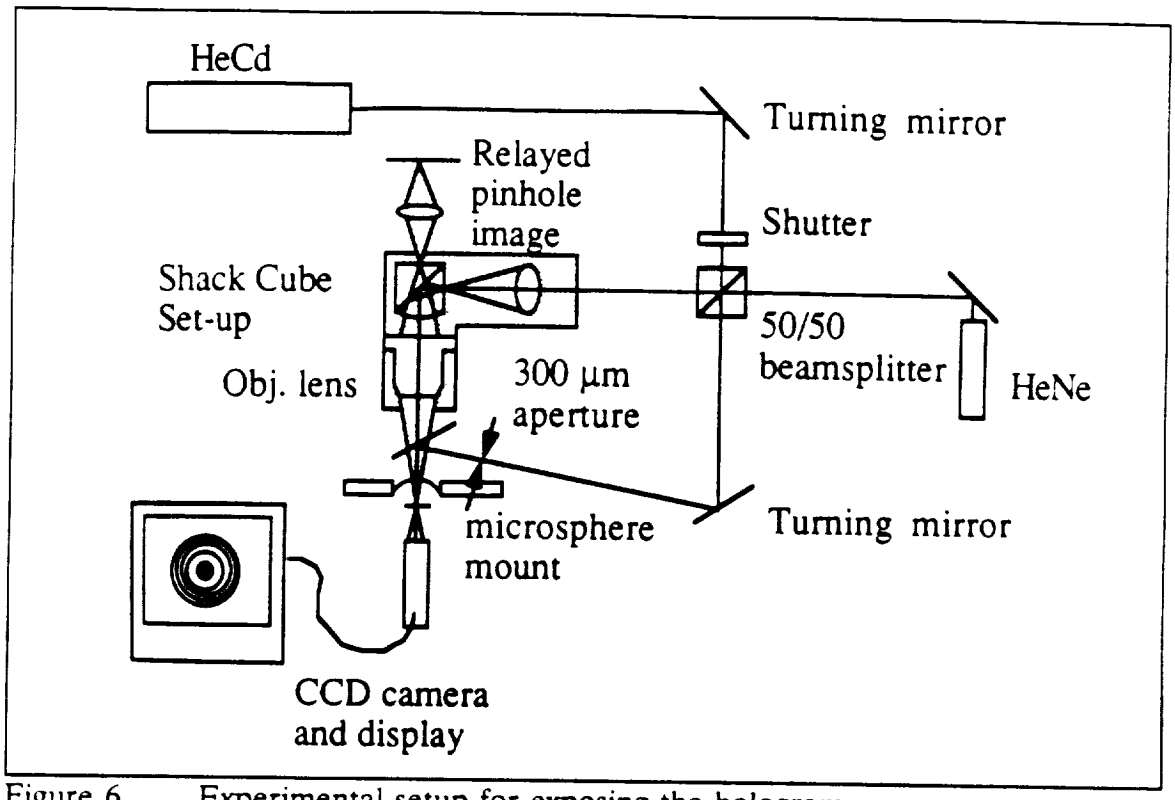


Figure 6. Experimental setup for exposing the hologram.

1000 μm range. The shells are 1 μm to 3 μm thick. We have measured quality of two microspheres using a ZYGO interferometer. Initial tests have shown that the parallelism between the inner and outer surfaces is better than a fraction of a fringe. The wavefront quality of the surfaces varies dramatically. One sphere tested with the ZYGO was of sufficient quality to use as a substrate, and the other was not. We visually inspect the surface before each attempt at making a lens.

Our construction procedure consists of making a holographic exposure from a converging beam and a planar wavefront. A modified Mach-Zehnder arrangement was used, which is similar in principle to one described by Nishihara and Suhara (11). The experimental setup is shown in Figure 6. A HeCd laser was used to expose the photoresist, and a HeNe laser was used for alignment. Both lasers were aligned to be coaxial. A shutter controlled light from the HeCd laser. One arm of the interferometer passed through a Shack-cube beam splitter that provided the object point for a finite-conjugate objective lens. The objective lens was focused at the center of curvature of the microsphere. The second arm of the interferometer was reflected off a turning mirror and a pellicle beam splitter to provide the plane-wave component for the hologram. Fringes were observed by a CCD camera behind the microsphere mount. Reflections off the microsphere that passed back through the Shack cube were used to align the substrate axially and transversely. After aligning with the HeNe laser, the substrate was translated axially the proper distance to compensate for focal shift caused by the blue HeCd laser.

Tolerance of the construction process is an important part of this study. We used CODEV, an optical design program, to study tolerances for $f$= 0.50 mm, NA = 0.50 and $\lambda$ = 0.442 μm. Transverse displacement and axial defocus errors during the construction process

MILSTER

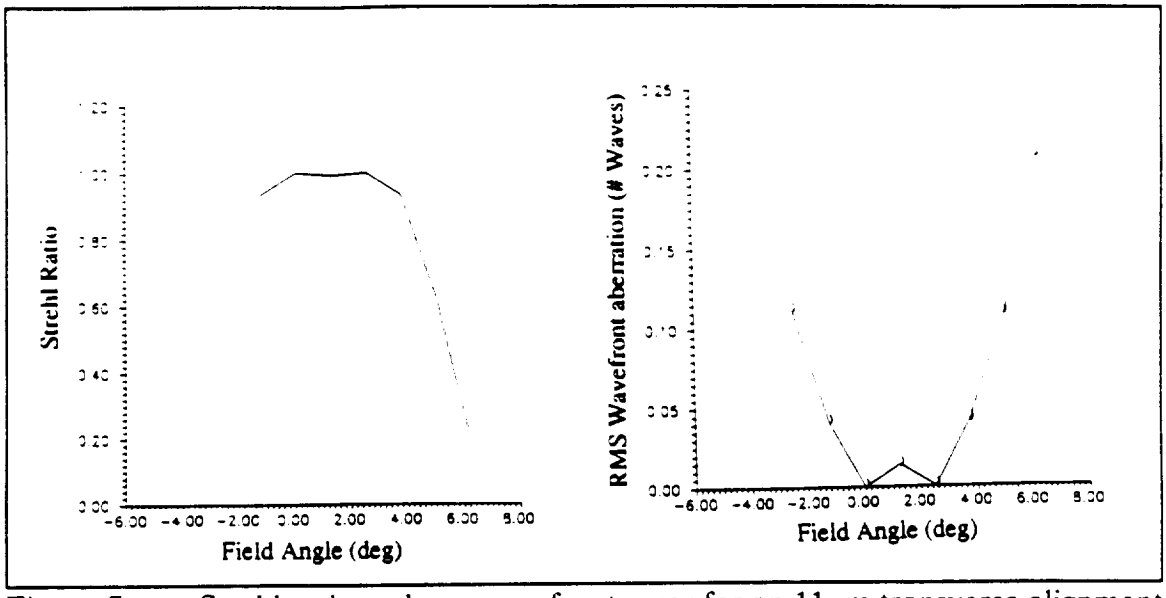


Figure 7. Strehl ratio and rms wavefront error for an 11$\mu$m transverse alignment error.

were studied. The Strehl ratio and rms wavefront error are displayed in Figure 7 for an 11 $\mu$m transverse alignment error. The useful field angle is $\pm 2.6^{\circ}$ centered about $1.3^{\circ}$. The rms wavefront aberration indicates that there are two fields angles for which aberration is essentially zero. Figure 8 displays astigmatic line images versus field angle. Since there is no coma in this system, the line image plot is a good indicator of how the device would actually perform. There are two points in the field where the astigmatism is zero. This indicates that the system behaves with binodal astigmatism. The transverse displacement can be compensated by tilting the lens to the appropriate bias angle. Strehl ratio and

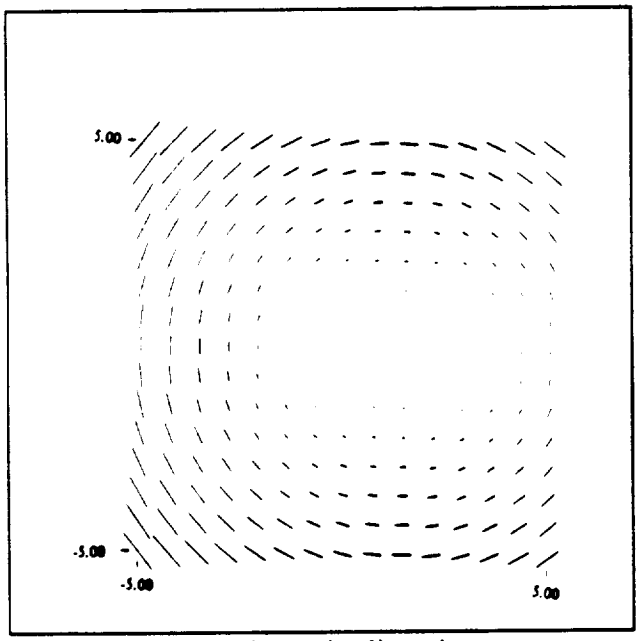

Figure 8. Astigmatic line images versus field angle.

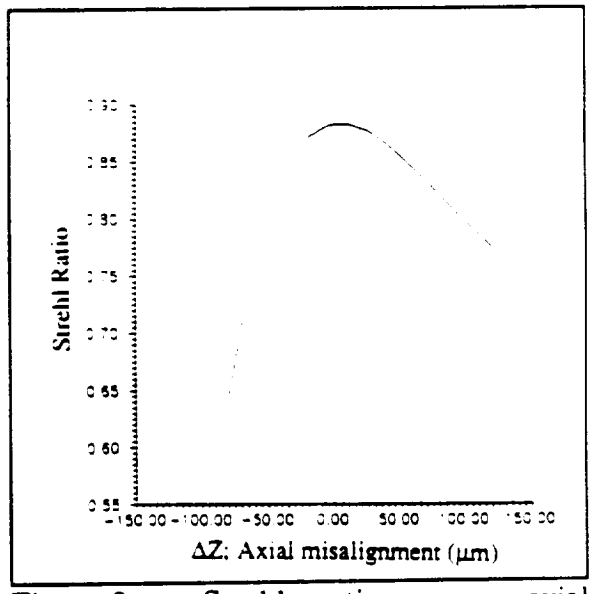


Figure 9. Strehl ratio versus axial alignment error.



MILSTER

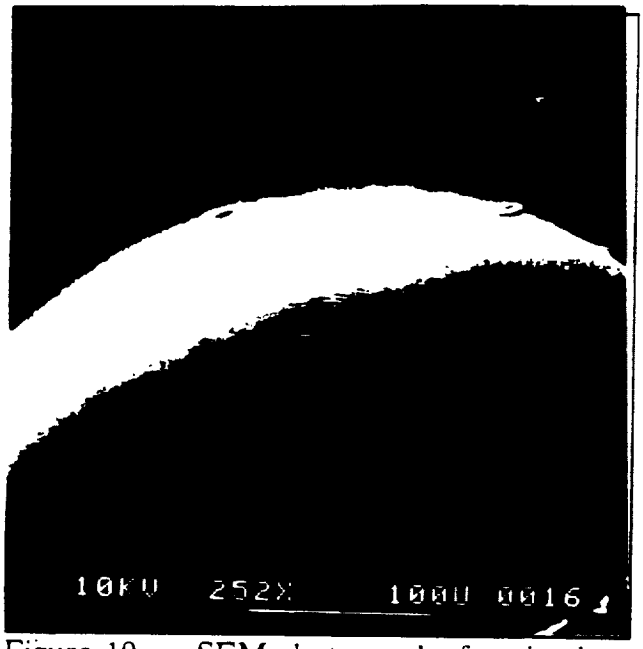


Figure 10. SEM photograph of a microlens exposed on a curved substrate.

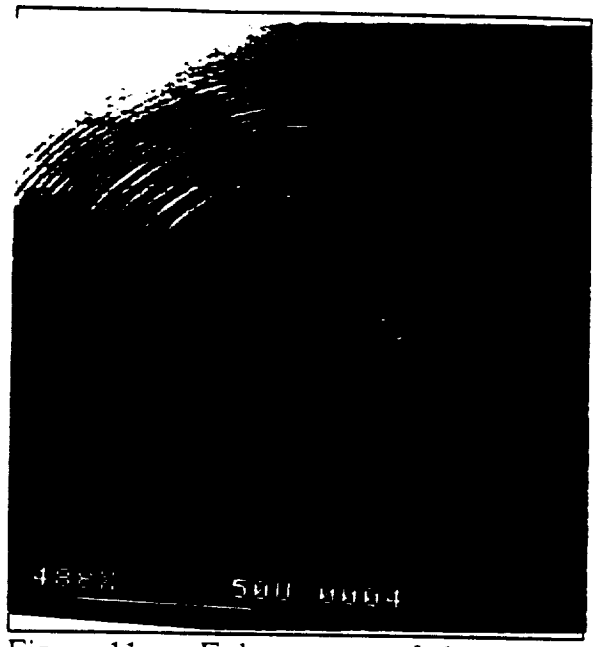


Figure 11. Enlargement of the central portion of Figure 10.

versus axial alignment error is shown in Figure 9. The allowable defocus is in the range of $\pm 30$ $\mu$m, which is quite easy to control.

## 5. Results

A standard photoresist solution was used to coat a microsphere. The microsphere was cut in half and mounted on a holder. Figure 10 shows an SEM photograph of a microlens that has been exposed on the curved surface. We were only able to expose a 0.16 NA lens due to a conflict between the finite working distance of the objective lens and the pellicle beam splitter. Figure 11 shows the same lens under higher magnification. A rough appearance is observed in the holographic pattern.

We tried to test the optical quality of the microlens, but, due to the large amount of scatter, strong zero-order beam, and small size, we were not able to get consistent results. We did test diffraction efficiency and lens NA, which were 11.8% and 0.16, respectively.

## 6. Conclusions

We have shown that, in order for micro optics to be used effectively in advanced data storage systems, off-axis aberrations must be considered. One solution for improving off-axis performance is to curve the substrate of a MFL so that its radius of curvature is equal to its focal length. This satisfies the Abbe sine condition, and effectively eliminates coma. We tried a proof-of-principle experiment in which a microsphere substrate was coated with photoresist and exposed in a modified Mach-Zehnder interferometer. We were successful in exposing a 0.16 NA photoresist pattern. The pattern was mottled, so we were not able to test the lens quality due to scattering and physical constraints. The holographic method was instructive, but the NA is limited to rather low values (<0.20). Our group is pursuing

MILSTEN

other methods of writing the patterns, which include electron-beam writing and binary optics.

## 7. Acknowledgements

This work was supported by the Optical Data Storage Center and the Joint Services Optical Program. Bob Trusty, who received his master's degree from this project, was supported by a graduate fellowship from Lawrence Livermore National Laboratories.

## 8. References

1. Corning, Inc., commercial literature describing model 350160 aspheric lens.
2. G.L. Lawrence and P.J. Cronkite, "Waveguide grating with broad spectral response using gradient-effective index," University of Arizona patent disclosure submitted June 6, 1988.
3. K. Iga, Y. Kokuban, M. Oikawa, *Fundamentals of Microoptics,* Academic Press, New York, 1984.
4. G.T. Sincerbox, "Miniature optics for optical recording, " *Proceedings of the SPIE*, vol. 935, Gradient-Index Optics and Miniature Optics, pp. 63-76 (1988).
5. H. Nishihara and T. Suhara, "Micro Fresnel Lenses," in *Progress in Optics Vol XXIV,* E. Wolf, ed., North-Holland Physics Publishing, New York, pp. 3-36 (1987)
6. M. Young, "Zone plates and their aberrations," JOSA, vol. 62, No. 8, pp. 972-976 (1972)
7. R. Kingslake, *Lens Design Fundamentals,* Academic Press, Inc., San Diego, p. 158 (1978)
8. W.T. Welford, "Aplanatic hologram lenses on spherical surfaces," Opt. Com., vol. 9, no. 3, p. 268-269 (1973).
9. E. Delano, "Primary aberrations of meniscus Fresnel lenses," JOSA, vol. 66, No. 12, pp 1317-1320 (1976).
10. H. Dammann, "Blazed Synthetic Phase-Only Holograms," Optik, vol 31, pp. 95-104 (1970)
11. N. Nishihara and T. Suhara, "Micro Fresnel lenses," Progress in Optics V XXIV, E. Wolf, editor, North-Holland Physics Publishing, New York, pp. 3-35 (1987).

MILSTER